The developing flow characteristics of water - ethylene glycol mixture based Fe_3O_4 nanofluids in eccentric annular ducts in low temperature applications

Nur Çobanoğlu [a],[*], Alireza Banisharif [b], Patrice Estellé [c], Ziya Haktan Karadeniz [d]

[a] Graduate School of Natural and Applied Sciences, İzmir Kâtip Çelebi University, 35620, İzmir, Turkey
[b] Chimie-Physique (MRC), Université Libre de Bruxelles, 1050, Brussels, Belgium
[c] Univ Rennes 1, LGCGM, 35704 Rennes, France
[d] Department of Energy Systems Engineering, İzmir Institute of Technology, 35430, İzmir, Turkey

ARTICLE INFO

ABSTRACT

Natural circulation loops with double pipe heat exchangers at heating and cooling ends have a potential to be used in the refrigeration systems as an alternative to suction line heat exchangers. The heat transfer capability of such natural circulation loops depends on the geometrical parameters as well as thermophysical properties of the working fluid. This study aims to investigate the effect of water-ethylene glycol mixture based Fe_3O_4 nanofluids (0.01, 0.05 and 0.1 vol.%) on the annular flow propagation and heat transfer in the annuli of double pipe heat exchanger at low pressure side of the refrigeration cycle. In addition to increased non-dimensional velocity values due to the lower viscosity and higher non-dimensional temperature values with expanded temperature gradient, improved heat transfer by nanofluids shows that they can be used as secondary heat transfer fluids at low-pressure side in refrigeration systems. Although the maximum transferred (13.6% improvement compared to base fluid) heat observed for the highest concentration, the nanofluids with smallest concentration has the minimum pressure drop value (25% reduction compared to base fluid) and the highest performance evaluation criteria (PEC) value (PEC = 1.08) with tiny increase in exergy destruction (1.45% compared to base fluid).

1. Introduction

Rapid growth of energy demand requires passive heat transfer techniques to recover, transfer and use of generated heat to improve energy efficiency and reduce energy consumption. Since household refrigeration appliances comprise a large portion of buildings' energy consumption [1], energy efficient solutions are proposed for vapor compression systems. Suction line heat exchangers (SLHXs) are generally used to increase system capacity and protect the components of the vapor compression systems by subcooling the refrigerant at high-pressure side and superheating at the low-pressure side. Reduction in the temperature at the condenser outlet results in lower enthalpy of evaporator inlet and thus higher evaporator capacity. In addition to increasing system performance, SLHXs have the advantages of that flash gas formation at the expansion device inlet can be prevented by subcooling of the refrigerant and fully evaporation of the liquid is obtained in the suction line prior to reaching the compressor [2]. However,

increase in temperature at the compressor inlet leads lower compressor efficiency and reduction in the system performance [3,4]. In addition to these two aspects, design and dimensions of SLHX have a great importance in the applications [5].

Single-phase natural circulation loop (SPNCL), as passive heat transfer system, was proposed as an alternative to suction line heat exchangers in vapor compression systems [6]. Using SPNCLs with double pipe heat exchangers (DPHXs) at low-pressure side and high-pressure sides of an existing refrigeration cycle does not require any changes in the pipeline of the cycle. The heat required for subcooling, and superheating processes is transferred between refrigerant and secondary heat transfer fluid flowing through annuli of DPHXs of a SPNCL. This provides more flexibility in the design of the system compared to the conventional SLHX in which the condenser outlet and suction line pipes are connected by internal heat exchangers.

DPHX, as the simplest form of a two-fluid heat transfer device, is comprised by two concentric circular tubes which presents circular and annular duct flow geometries [7]. The annular channel of a DPHX might

---

Nomenclature

3D	Three dimensional
c_p	Specific heat (J/kg.K)
D_i	Inner pipe diameter (m)
D_o	Outer pipe diameter (m)
e	Eccentricity (m)
e*	Dimensionless eccentricity
f	Friction factor
g	Gravitational acceleration (m/s^2)
h	Enthalpy (m^2/s^2)
k	Thermal conductivity of the working fluid (W/mK)
L_c	Length (m)
L^+	Dimensionless duct length
$\dot{m}$	Mass flow rate (kg/s)
Nu	Nusselt number
p	Pressure (Pa)
PEC	Performance Evaluation Criteria
Pr	Prandtl number
Q	Transferred heat (W)
q''	Heat flux (W/m^2)
r	Pipe radius (m)
r*	Pipe diameter ratio
Re	Reynolds number
S_M	Source of momentum (kg m^2/s^2)
S_E	Source of energy (kg m/s^3)
SPNCLs	Single phase natural circulation loops
$\dot{S}_{gen}$	Entropy generation (W/K)
$\dot{Ex}_{dest}$	Exergy destruction (W)

T	Temperature (K)
U	Overall heat transfer coefficient (W/m^{2}K)
$\vec{U}$	Velocity vector (m/s)

Greek Symbols

ρ	Density (kg/m^3)
β	Thermal expansivity (1/K)
φ	Volumetric concentration
μ	Viscosity (Pa.s)
ε	Aspect ratio
δ	Kronecker delta function
τ	Stress tensor

Subscriptions

a	Ambient
bf	Base fluid
c	Cooler
e	Effective
f	Fluid
FF	Flow friction
HT	Heat transfer
i	Inner
in	Inlet
LMTD	Logarithmic mean temperature difference
max	Maximum
nf	Nanofluid
o	Outer
p	Particle

be concentric or eccentric depending on the application, and the effects of eccentricity, pipe diameter, thermal boundary conditions and flow characteristics such as fully developed and developing flow on the heat transfer performance have been studied previously [7–9]. The effects of the passive heat transfer enhancement techniques are widely studied [10–12] and recent studies focus on the influence of the external magnetic field [13–16] on DPHXs performance. Additionally, thermophysical properties of working fluid can be considered as important parameters for the prediction of the heat transfer performance of DPHXs.

Nanofluids are also widely used in the DPHX as a working fluid for either in the annulus or inner tube. Togun et al. [17] compiled the studies on forced, natural and mixed convection in the annular passage for fluids and nanofluids and reported that nanofluids have higher heat transfer capability due to their thermophysical properties. Recently, Subramanian et al. [18] studied water based TiO$_2$ nanofluid in double-pipe counter-flow heat exchanger for laminar, transition and turbulent flows. They obtained up to 15% improvement in heat transfer coefficient by using nanofluids compared to the base fluid. Increase in concentration and Reynolds numbers boost the heat transfer of nanofluids. Khanlari et al. [19] found a maximum heat transfer coefficient by 37% and 12% for kaolin-deionized water based counter flow concentric tube and parallel flow concentric tube heat exchangers working under turbulent flow. Arya et al. [20] also investigated the heat transfer and pressure drop characteristics of ethylene glycol based MgO nanofluid in DPHX and found that heat transfer enhancement was obtained by 27% with the penalty of pressure drop increment by 35% for concentration of 0.3 wt.%. Shahsavar et al. [21] evaluated the hydrothermal performance of a hybrid nanofluid (water based tetramethylammonium hydroxide-coated Fe$_3$O$_4$ and gum arabic-coated carbon nanotube hybrid nanofluid) in a counter-current mini channel DPHX. They found that non-Newtonian hybrid nanofluid generally has a higher heat transfer

rate and thus overall heat transfer coefficient and effectiveness compared to Newtonian hybrid nanofluid. However, the Newtonian hybrid nanofluid exhibits higher pressure drop, pumping power, and performance evaluation criterion (PEC). Moreover, the impact of nanoparticle shapes on thermohydraulic performance of minichannel DPHX working with water-ethylene glycol based boehmite alumina nanofluids was investigated in [22]. It was shown in this study that platelet shaped nanofluids have better heat transfer characteristics whereas spherical shaped nanofluids demonstrated higher performance index. Jassim and Ahmed [23] studied water based Al$_2$O$_3$ and Cu nanofluids in DPHX, and found that Cu nanofluid has higher enhancement in Nusselt numbers (23% for Cu and 13% for Al$_2$O$_3$ respectively) and considerable improvement in effectiveness (10% for Cu and 7% for Al$_2$O$_3$ respectively). Additionally, the Al$_2$O$_3$ nanofluid demonstrated higher heat leak compared to Cu nanofluid. In their comprehensive review study, Omidi et al. [24] mentioned that combination of nanofluids and passive heat transfer methods in DPHXs would be a solution of many heat transfer problems which is widely studied in the current literature.

The increase in performance of heat transfer systems has been generally associated with the improvement in the thermophysical properties of nanofluids compared to base fluids [25–27]. Although addition of nanoparticles in base fluids generally results in increase of viscosity [28, 29], decrease of viscosity could also be obtained by increasing particle size [30], and lubricating effect [31,32] depending on nanoparticle content and generally obtained at small concentrations [33]. Since higher viscosity values require higher pumping power [34–37], recent studies show that nanofluids have a potential in passive heat transfer systems where there is no pump driven motion of the liquid [38]. In the low temperature applications, such as refrigeration systems, water - ethylene glycol mixture (WEG) is used as the working fluid of the DPHXs to improve heat transfer considering the freezing temperature limitation of water. Recently, Banisharif et al. [33] studied the
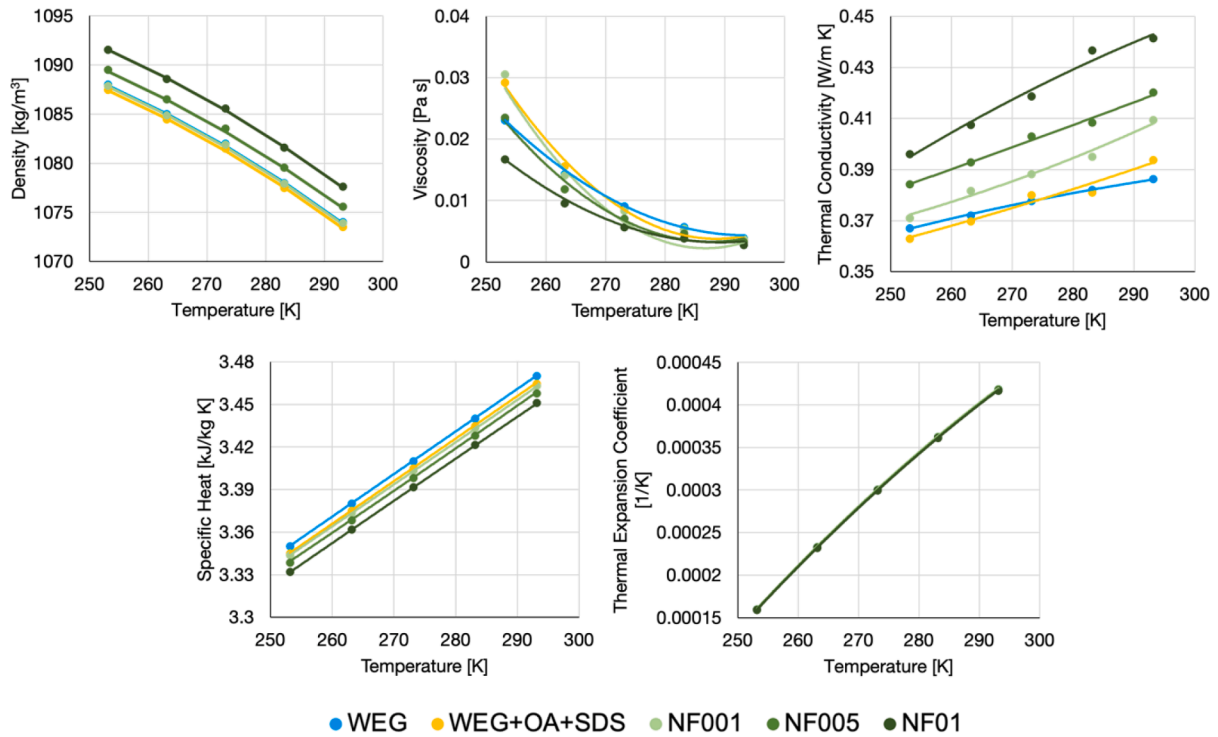
Fig. 1. The variation of the thermophysical properties of base fluid and nanofluids with temperature.

thermophysical properties of WEG (50:50) based Fe_3O_4 nanofluids at low concentration (0.01, 0.05 and 0.1 vol.%) and temperatures (253.15–293.15 K). It is found that increase of nanoparticle concentration resulted in higher thermal conductivity and lower viscosity values which would affect the heat transfer enhancement in passive systems positively.

Considering the lower viscosity values in the passive heat transfer systems, this study investigates the potential of WEG based nanofluids in the low-pressure side of vapor-compression system assisted with SPNCL. In the proposed system, the nanofluids in annular section are considered as secondary fluid for superheating the refrigerant which flows through the inner pipe of the DPHX. A 3D transient numerical model has been developed to understand laminar annular flow propagation of nanofluids. The effect of WEG based nanofluids' lower viscosity values on the DPHX performance is evaluated in terms of temperature and velocity distributions, thermohydraulic performance, exergy destruction and entropy generation analyses.

2. Materials and methods

2.1. Thermophysical properties

Banisharif et al. [33] used a mixture of WEG (50:50) as a basefluid at 293.15 K with the amount of 0.2 wt.% in sodium dodecyl sulfonate (SDS) and 0.2 vol.% in oleic acid (OA) to disperse and stabilize Fe_3O_4 nanoparticles. WEG, WEG+OA+SDS and Fe_3O_4 nanofluid (0.01, 0.05 and 0.1 vol.%) were used as working fluids in this study. The thermophysical properties, namely thermal conductivity, heat capacity, dynamic viscosity and density, presented in [33] was introduced to numerical model as polynomials which are function of temperature. The reader is refereed to ref. [33] for the full description of nanofluid preparation and characterization, as well as discussion of the results. Beside these experimental data [33], the effective thermal expansion coefficient (β_e)of the working fluids was calculated by mixture rule in Eq. (1) and Eq. (2). In those equations, φ denotes volumetric concentration of the nanofluid and ρ is the density. Subscripts p and f are for nanoparticle and fluid, respectively. For the WEG (50:50) calculation in

Eq.(1), temperature dependent thermal expansion coefficient of EG is obtained from [39] and tabular values of water were used [40]. Then, the calculated thermal expansion coefficient of WEG was used in Eq. (2) for Fe_3O_4 nanofluids. The constant value of 1.13×10^{-5} was used for the thermal expansion coefficient of Fe_3O_4 [41] by assuming the WEG's temperature dependency as the dominant parameter. The variation of thermophysical properties with temperature and nanoparticle content is presented in Fig. 1.

$$(\rho\beta)_e = (1 - \varphi_{water})(\rho\beta)_{water} + \varphi_{EG}(\rho\beta)_{EG} \tag{1}$$

$$(\rho\beta)_e = (1 - \varphi_f)(\rho\beta)_f + \varphi_p(\rho\beta)_p \tag{2}$$

2.2. Numerical model

Here, a transient 3D numerical model was used to study developing laminar flow characteristics and heat transfer capability of eccentric annular duct. A commercial software (ANSYS CFX) was used to build a geometry and solution of a steady laminar full buoyancy model with temperature dependent thermophysical properties. General form of the governing equations for steady state 3-D incompressible flow with negligible viscous dissipation can be expressed in Eq. (3)–(5) as [42],

$$\text{Mass conservation equation}: \nabla \cdot \left(\rho \overrightarrow{U} \right) = 0 \tag{3}$$

$$\text{Momentum equation}: \nabla \cdot \left(\rho \overrightarrow{U} \otimes \overrightarrow{U} \right) = -\nabla p + \nabla \cdot \tau + S_{M,buoyancy} \tag{4}$$

$$\text{Energy equation}: \nabla \cdot \left(\rho \overrightarrow{U} h \right) = \nabla \cdot (k \nabla T) + \overrightarrow{U} \cdot \nabla p + S_E \tag{5}$$

In the governing equations, h and $\overrightarrow{U}$ are enthalpy (m^2/s^2) and velocity vector (m/s). S denotes source of momentum ($kg\ m^2/s^2$) and energy ($kg\ m/s^3$). τ is stress tensor and given as,

$$\tau = \mu \left(\nabla \overrightarrow{U} + \left(\nabla \overrightarrow{U} \right)^T - \frac{2}{3} \delta \nabla \cdot \overrightarrow{U} \right) \tag{6}$$
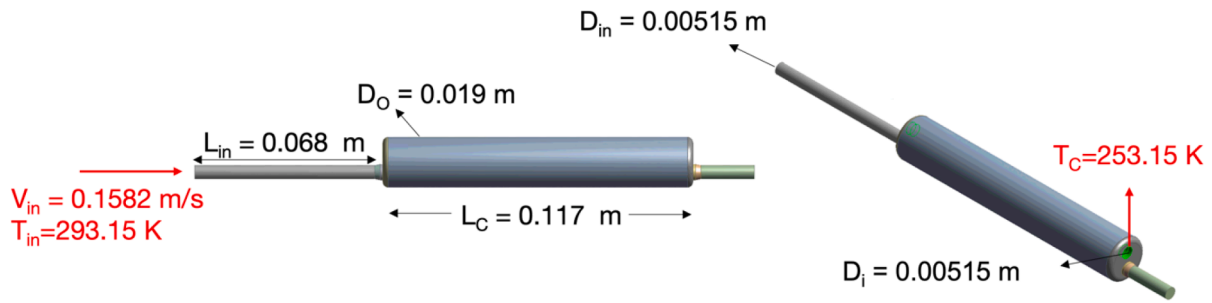
where δ is the Kronecker delta.

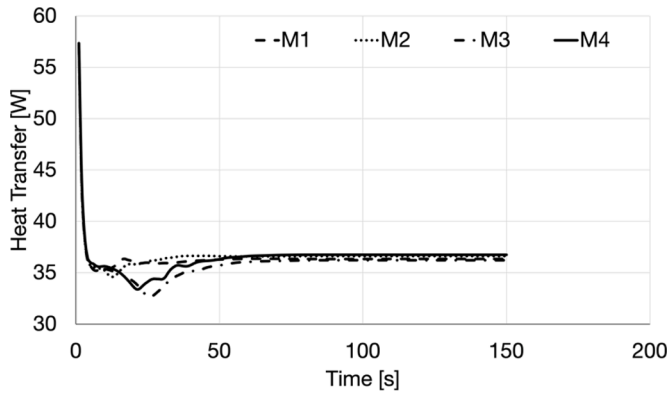**Fig. 2.** The boundary conditions and dimensions of the annular pipe.

Fig. 3. Mesh dependency results for sensitivity analysis.

Full buoyant method is determined in the numerical method as,

$$S_{M,buoyancy} = (\rho - \rho_{ref})g \tag{7}$$

Here ρ_{ref} is reference density of working fluid which is calculated at the average fluid temperature in the system.

In the system, which is created by using accessible parts of an existing cooling system, the pipes through which the refrigerant passes are the inner pipes of the DPHXs located at the cooling and heating-ends. In order to positively affect the heat transfer and flow progression, the inner pipe with 5.15 mm in diameter is located in the upper position on the cooling-end. The annular duct has 19 mm of outer diameter and 117 mm of length with an upstream calming length of 68 mm and diameter of 5.15 mm. The dimensionless eccentricity (e*) of the annular duct is calculated as 0.54 with the pipe diameter ratio (r*) 0.27. The refrigerant which has been supposed to flow through inner pipe of the duct was

introduced to system by employing lower constant temperature boundary condition ($T_C = 253.15$ K) at inner pipe as shown in Fig. 2. The primary working fluid flows through the annuli with the inlet velocity $V_{in} = 0.1582$ m/s at $T_{in} = 293.15$ K for 250 s with time step of 0.05 s. The inlet velocity is determined by the average velocity value at cooling-end inlet in SPNCL [6].

Four different meshes (M1, M2, M3, M4 having 156,247, 258,423, 434,597, and 612,463 elements respectively) were used for the mesh independency analysis of the numerical model working with WEG. Fig. 3 shows that M1&M2 cannot capture the unsteady initial behavior between 15 and 65 s which characteristically exists in DPHXs. However, M3 and M4 can distinguish this behavior. Therefore, M4 is used to evaluate temperature and velocity distributions at the critical cross-sections with high resolution.

The developing flow characteristics have been investigated considering the effects of nanofluid concentrations on nondimensional temperature (T*) and velocity (V*) distributions at critical cross-sections of the eccentric annular ducts.

$$T^* = \frac{T_s - T_{inlet}}{T_c - T_{inlet}} \tag{8}$$

$$V^* = \frac{V_s}{V_{inlet}} \tag{9}$$

Here, T_s and V_s are the local temperature [K] and velocity [m/s] values at these cross-sections.

Heat transfer performance of system is also evaluated by determining the Nusselt number (*Nu*):

$$Nu = \frac{U(D_o - D_i)}{k}, \tag{10}$$

The overall heat transfer coefficient (*U*) in Eq. (10) was evaluated by the logarithmic mean temperature difference (LMTD) and surface area
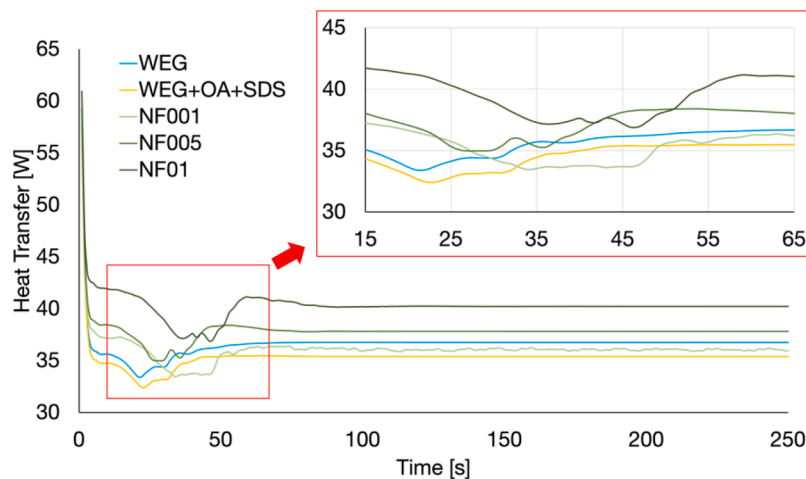

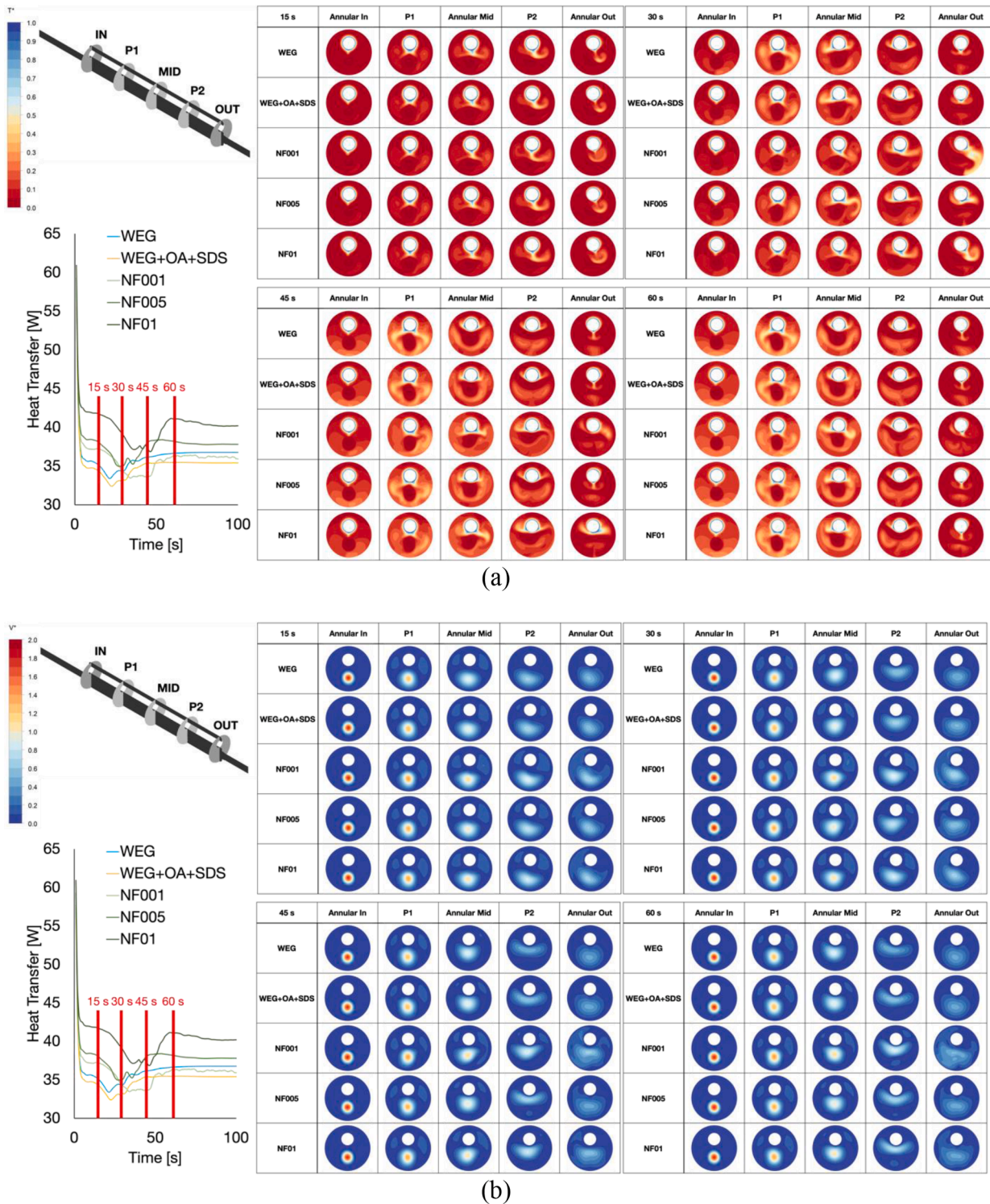**Fig. 4.** Time dependent variation of heat transfer.

4

Fig. 5. Cross-sectional (a) T* and (b) V* distributions between the time range of 15–65 s.

of the inner pipe. Overall heat transfer coefficient was calculated by using the equation below:

$$U = \frac{Q}{\pi \, D_i \, L_c \, \Delta T_{LMTD}}, \tag{11}$$

where,

$$\Delta T_{LMTD} = \frac{\Delta T_1 - \Delta T_2}{\ln(\Delta T_1 / \Delta T_2)}, \tag{12}$$

$$\Delta T_1 = T_{in} - T_c, \tag{13}$$

$$\Delta T_2 = T_{out} - T_c, \tag{14}$$

Reynolds number is determined by

$$Re = \frac{\rho V_{in}(D_o - D_i)}{\mu}, \tag{15}$$

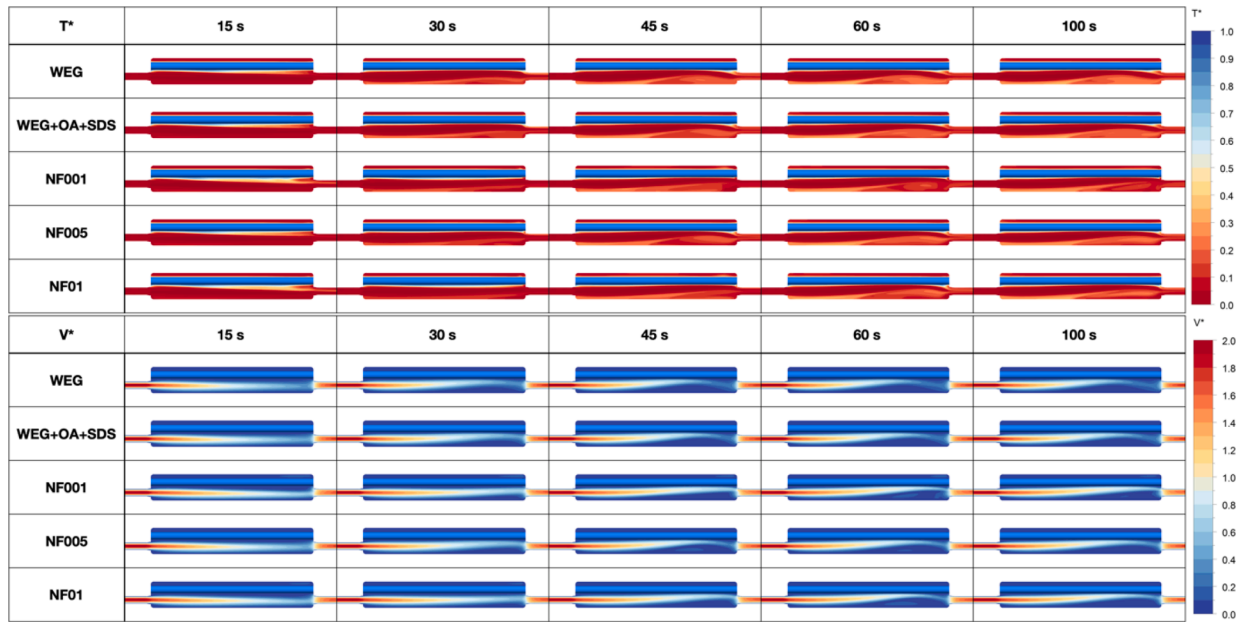The friction factor is calculated by using the model proposed for

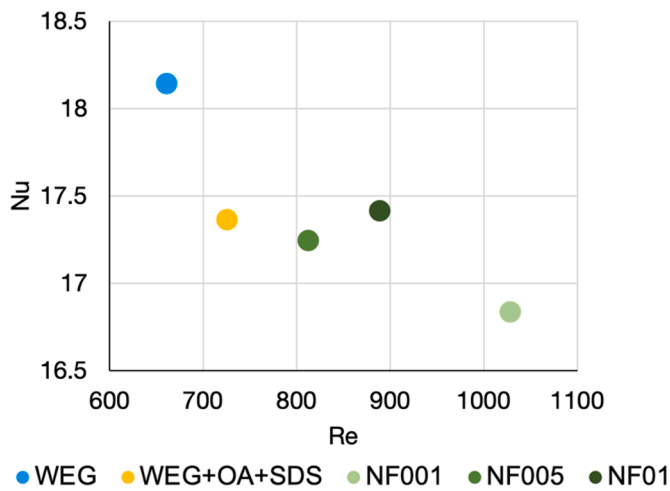**Fig. 6.** Axial distributions of the T* and V* along the annular duct.
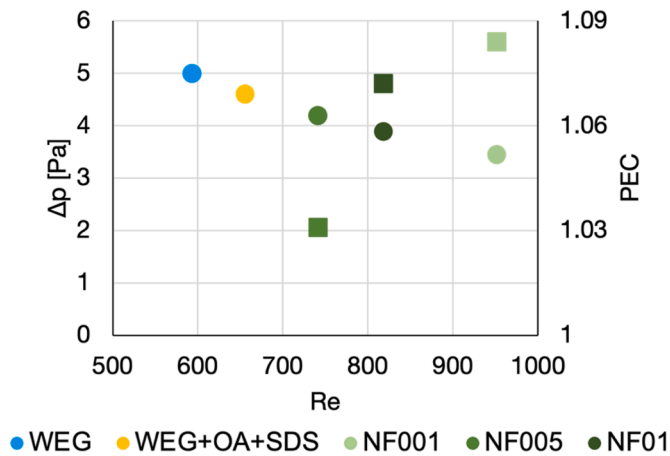

Fig. 7. Variation of Nu with *Re*.

Fig. 8. Variation of Δp and PEC with *Re* (circle and square markers indicate the Δp and PEC respectively).

developing laminar flow in eccentric annulus [43] and given by

$$fRe_{\sqrt{A}} = \left[\left(\frac{3.44}{\sqrt{L^+}} \right)^2 + \left(\frac{12}{\sqrt{\in} (1 + \in) \left[1 - \frac{192 \in}{\pi^5} \tanh\left(\frac{\pi}{2\in}\right) \right]} \right)^2 \right]^{1/2}, \quad (16)$$

Here, $\in$ is the aspect ratio and determined pipe diameter ratio (r* = D_i/D_o) and dimensionless eccentricity (e* = e / (r_o - r_i)) of the annulus.

$$\in = \frac{(1 + e^*)(1 - r^*)}{\pi(1 + r^*)}, \quad (17)$$

Moreover, L^+ in the Eq. (16) is defined as dimensionless duct length and given by

$$L^+ = \frac{\mu L_c}{\dot{m}}, \quad (18)$$

Pressure drop (Δp) through the annular duct is determined as follows

$$\Delta p = f \frac{L_c}{D_o - D_i} \frac{\rho V_{in}^2}{2}, \quad (19)$$

The performance evaluation criteria (PEC) of the system are calculated by using Nu and friction factor [18].

$$PEC = \frac{\frac{Nu_{nf}}{Nu_{bf}}}{\left(\frac{f_{nf}}{f_{bf}} \right)^{\frac{1}{3}}}, \quad (20)$$

The total entropy generation rate of the system consists of thermal and frictional entropy generations as given in Eq. (21) [44].

$$\dot{S}_{gen} = \left(\dot{S}_{gen} \right)_{HT} + \left(\dot{S}_{gen} \right)_{FF}, \quad (21)$$

where

$$\left(\dot{S}_{gen} \right)_{HT} = \frac{q''^2 \pi D_h^2}{kT^2 Nu(Re_D, Pr)}, \quad (22)$$

$$\left(\dot{S}_{gen} \right)_{FF} = \frac{8\dot{m}^3 f(Re_D)}{\pi \rho^2 T(D_o - D_i)^5} \quad (23)$$

The exery destruction is evaluated by

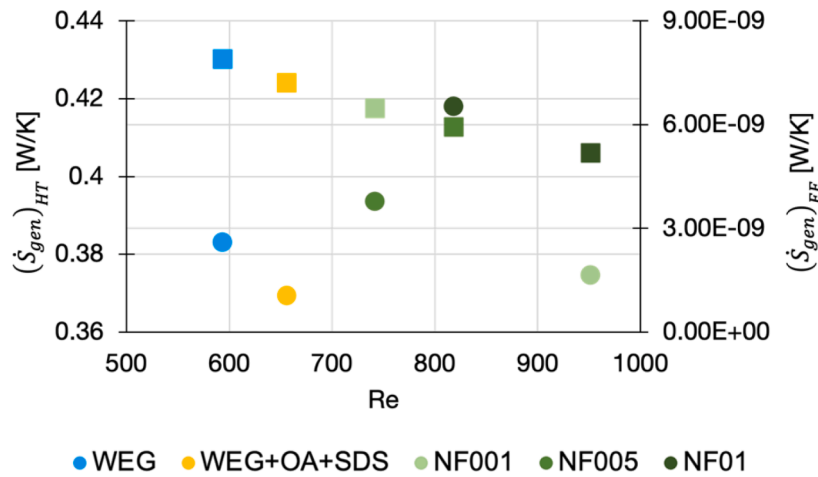$$\dot{Ex}_{dest} = T_a \dot{S}_{gen} \quad (24)$$

Fig. 9. Individual behavior of heat transfer and frictional components of total entropy generation rates (circle and square markers indicate the $(\dot{S}_{gen})_{HT}$ and $(\dot{S}_{gen})_{FF}$, respectively).
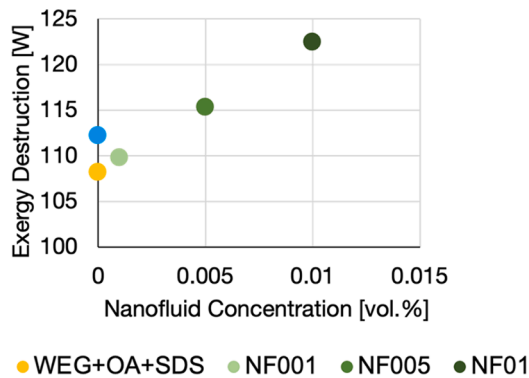

Fig. 10. Exergy destruction with nanofluid concentration.

Here T_a is the ambient temperature and it equals to T_{in} for this study.

3. Results and discussions

Since the effect of nanofluids on heat transfer performance at low-pressure side in refrigeration system is aimed to be investigated in this study, the change of heat transfer with time is evaluated in Fig. 4. In Fig. 4 and the following figures, NF001, NF005 and NF01 are expressed as nanofluids having 0.01, 0.05 and 0.1 of volumetric concentrations, respectively. The higher temperature difference between the inlet and the inner pipe results in higher heat transfer value at the beginning, but as time progress (to 15 s) drastically reduction in heat transfer is obtained for all working fluids. In the time range of 15–65 s, the heat transfer change is unstable, and it can be seen that increase in nanofluid concentration delays the time require to reach steady-state flow conditions.

Focusing on the time range of 15–65 s in which the fluctuations observed before steady-state condition, the heat transfer in annular duct is evaluated in terms of T* and V* at critical cross sections (Figs. 5 and 6). The cross-section P1 and P2 are at the middle of the first half and second half, respectively. Hot fluid entering the pipe results in hot fluid pocket at the wider section of the annular. Cross-sectional distributions of T* (Fig. 5) and axial distributions of T* and V* (Fig. 6) this hot pocket region continues through the middle section for all cases. As time progress, the higher T* value distribution, which means cooler fluid, is obtained near the inner pipe and it increases with nanofluid concentration. Additionally, higher T* area at the narrow section of the annular duct is obtained for the NF01 case (Fig. 6). V* increases with nanofluid

concentration and the velocity of the entering hot fluid decreases along the annulus and flow through the uppermost region of annular (Figs. 5b and 6). This behavior enables to distribution of cold fluid in the wider region of annular and thus mixing of warm and cold fluid as shown in the cross-sections of P2 and out presented in Fig. 5.

Additionally, the heat transfer performance is evaluated by variation of Nu number by *Re*. Fig. 7 shows that WEG has highest Nu number, and it decreases slightly for WEG+OA+SDS and nanofluid cases. However, the *Re* changes independently from the concentration of the nanofluids due to the nonlinear variation of the viscosity values (Fig. 1). Manglik and Fang [7] investigated the effects of eccentricity and boundary conditions on the fully developed laminar annular flow for different pipe diameter ratios. Focusing on the similar eccentricity and pipe diameter ratio values in this study, they found that Nu number varies in the range of 4.769 and 4.998 for the fully developed flow in the annular duct under having the 0.25 of pipe diameter ratio and 0.4–0.6 of eccentricity limits, respectively. This range is valid for constant temperature boundary condition at inner tube and adiabatic wall of outer tube. The Nu numbers found in our study are higher than Manglik and Fang [7]. The possible reason behind this could be our geometry. In the most of the annular duct studies, the working fluid enters the annular duct directly from annuli region. However, it enters partially from a tube with smaller diameter (5.15 mm) in our geometry. This affects the flow propagation through the annuli region as shown in Figs. 5 and 6.

Since the DPHX is aimed to superheat the refrigerant at the low-pressure side of refrigeration cycle, the transferred heat is investigated for all cases. Although, addition of the OA and SDS reduces the transferred heat, heat transfer increases (by 13.6% for NF01 compared to WEG+OA+SDS as a basefluid) for the nanofluids (35.53 W, 34.22 W, 34.75 W, 36.55 W and 38.89 W for WEG, WEG+OA+SDS, NF001, NF005 and NF01 respectively). In addition to increased V* values due to the lower viscosity and higher T* values with expanded temperature gradient, improved heat transfer by nanofluids shows that they can be used as secondary heat transfer fluids at low-pressure side in refrigeration systems.

The Δp decreases with the increasing Reynolds number, and nanofluids have smaller values compared to base fluid because of lower viscosity of nanofluids. The nonlinearity in the viscosity behavior for the investigated concentrations also affects the Δp values because of its dependency on the friction factor. Additionally, the PEC values of the nanofluids have been determined by assuming the WEG+OA+SDS as base fluid (Fig. 8). Considering the tiny changes in Nu numbers in Fig. 7, smaller pressure drops of nanofluids results in PEC > 1 for all cases which means that the improvement of heat transfer is larger than the increase in the pressure drop penalty. The nanofluid with the smallest

concentration (NF001) has the smallest pressure drop value of 3.88 Pa with 1.08 of PEC value.

Fig. 9 shows that the effect of surfactant utilization with WEG reduces the $(\dot{S}_{gen})_{HT}$ but then addition of the nanoparticles causes the irreversibilities and thus higher $(\dot{S}_{gen})_{HT}$ (up to 11% for NF01 compared to WEG+OA+SDS). Although there is no significant difference between inlet and outlet temperatures, greater values of transferred heat results in higher values of entropy generation. On the other hands, frictional entropy generation rates decrease with the increase of *Re* but they are too small to be taken into consideration.

Considering the negligible value of $(\dot{S}_{gen})_{FF}$, the exergy destruction strongly depends on the transferred heat in $(\dot{S}_{gen})_{HT}$ (Eq. (22)) compared to other parameters (Nu, T, k) for this study. Increase in transferred heat for higher nanofluid concentrations results in higher exergy destructions as shown in Fig. 10.

4. Conclusions

In this study, we evaluated the effects of WEG based Fe$_3$O$_4$ nanofluids on the annular flow propagation and temperature distribution in the annuli of double pipe heat exchanger at low pressure side of the refrigeration cycle. It is found that utilization of nanofluids have wider T* distribution at higher values which means increased cooler region and higher V* compared to WEG and WEG+OA+SDS. Although addition of the nanoparticles results in delay to reach steady-state conditions, heat transfer increases up to 13.6% compared to WEG+OA+SDS as a basefluid. Although the highest transferred heat observed for NF01 case, NF001 has the smallest pressure drop value and exergy destruction with the highest PEC value. The results show that nanofluids improved the heat transfer at low-pressure side of the refrigeration system.

Declaration of Competing Interest

The authors declare that they have no known competing financial interests or personal relationships that cdocould have appeared to influence the work reported in this paper.

Acknowledgement

References

[1] J.M. Belman-Flores, J.M. Barroso-Maldonado, A.P. Rodríguez-Muñoz, G. Camacho-Vázquez, Enhancements in domestic refrigeration, approaching a sustainable refrigerator–a review, Renew. Sustain. Energy Rev. 51 (2015) 955–968.

[2] S.A. Klein, D.T. Reindl, K. Brownell, Refrigeration system performance using liquid-suction heat exchangers, Int. J. Refrig. 23 (8) (Dec. 2000) 588–596, https://doi.org/10.1016/S0140-7007(00)00008-6.

[3] C. Park, H. Lee, Y. Hwang, R. Radermacher, Recent advances in vapor compression cycle technologies, Int. J. Refrig. 60 (2015) 118–134.

[4] R. Mastrullo, A. Mauro, S. Tino, G. Vanoli, A chart for predicting the possible advantage of adopting a suction/liquid heat exchanger in refrigerating system, Appl. Therm. Eng. 27 (14–15) (2007) 2443–2448.

[5] D. Sánchez, J. Patiño, R. Llopis, R. Cabello, E. Torrella, F.V. Fuentes, New positions for an internal heat exchanger in a CO2 supercritical refrigeration plant. Experimental analysis and energetic evaluation, Appl. Therm. Eng. 63 (1) (2014) 129–139.

[6] N. Çobanoğlu, H.D. Koca, A.M. Genç, Z.H. Karadeniz, O. Ekren, Investigation of performance improvement of a household freezer by using natural circulation loop, null (Jul. 2020) 1–13, https://doi.org/10.1080/23744731.2020.1798710.

[7] R. Manglik, P. Fang, Effect of eccentricity and thermal boundary conditions on laminar fully developed flow in annular ducts, Int. J. Heat Fluid Flow 16 (4) (1995) 298–306.

[8] E.E. Feldman, R.W. Hornbeck, J.F. Osterle, A numerical solution of developing temperature for laminar developing flow in eccentric annular ducts, Int. J. Heat Mass Transf. 25 (2) (1982) 243–253, https://doi.org/10.1016/0017-9310(82)90010-2.

[9] E.E. Feldman, R.W. Hornbeck, J.F. Osterle, A numerical solution of laminar developing flow in eccentric annular ducts, Int. J. Heat Mass Transf. 25 (2) (1982) 231–241, https://doi.org/10.1016/0017-9310(82)90009-6.

[10] S. Liu, M. Sakr, A comprehensive review on passive heat transfer enhancements in pipe exchangers, Renew. Sustain. Energy Rev. 19 (2013) 64–81.

[11] W. Wang, Y. Zhang, K.-.S. Lee, B. Li, Optimal design of a double pipe heat exchanger based on the outward helically corrugated tube, Int. J. Heat Mass Transf. 135 (2019) 706–716.

[12] S.S. Mousavi Ajarostaghi, M. Zaboli, H. Javadi, B. Badenes, J.F. Urchueguia, A review of recent passive heat transfer enhancement methods, Energies 15 (3) (2022), https://doi.org/10.3390/en15030986.

[13] A. Shakiba, K. Vahedi, Numerical analysis of magnetic field effects on hydrothermal behavior of a magnetic nanofluid in a double pipe heat exchanger, J. Magn. Magn. Mater. 402 (2016) 131–142, https://doi.org/10.1016/j.jmmm.2015.11.039.

[14] S.V. Mousavi, M. Sheikholeslami, M.B. Gerdroodbary, The influence of magnetic field on heat transport of magnetic nanofluid in a sinusoidal double pipe heat exchanger, Chem. Eng. Res. Des. 113 (2016) 112–124.

[15] M. Bahiraei, M. Hangi, Investigating the efficacy of magnetic nanofluid as a coolant in double-pipe heat exchanger in the presence of magnetic field, Energy Convers. Manag. 76 (Dec. 2013) 1125–1133, https://doi.org/10.1016/j.enconman.2013.09.008.

[16] P. Barnoon, D. Toghraie, F. Eslami, B. Mehmandoust, Entropy generation analysis of different nanofluid flows in the space between two concentric horizontal pipes in the presence of magnetic field: single-phase and two-phase approaches, Comput. Math. Appl. 77 (3) (Feb. 2019) 662–692, https://doi.org/10.1016/j.camwa.2018.10.005.

[17] H. Togun, T. Abdulrazzaq, S. Kazi, A. Badarudin, A. Kadhum, E. Sadeghinezhad, A review of studies on forced, natural and mixed heat transfer to fluid and nanofluid flow in an annular passage, Renew. Sustain. Energy Rev. 39 (2014) 835–856.

[18] R. Subramanian, A.S. Kumar, K. Vinayagar, C. Muthusamy, Experimental analyses on heat transfer performance of TiO 2–water nanofluid in double-pipe counter-flow heat exchanger for various flow regimes, J. Therm. Anal. Calorim (2019) 1–10.

[19] A. Khanlari, D. Yılmaz Aydın, A. Sözen, M. Gürü, H.İ. Variyenli, Investigation of the influences of kaolin-deionized water nanofluid on the thermal behavior of concentric type heat exchanger, Heat Mass Transfer 56 (5) (May 2020) 1453–1462, https://doi.org/10.1007/s00231-019-02764-1.

[20] H. Arya, M. Sarafraz, O. Pourmehran, M. Arjomandi, Heat transfer and pressure drop characteristics of MgO nanofluid in a double pipe heat exchanger, Heat Mass Transfer 55 (6) (2019) 1769–1781.

[21] A. Shahsavar, A. Godini, P.T. Sardari, D. Toghraie, H. Salehipour, Impact of variable fluid properties on forced convection of Fe 3 O 4/CNT/water hybrid nanofluid in a double-pipe mini-channel heat exchanger, J. Therm. Anal. Calorim. 137 (3) (2019) 1031–1043.

[22] A. Shahsavar, Z. Rahimi, H. Salehipour, Nanoparticle shape effects on thermal-hydraulic performance of boehmite alumina nanofluid in a horizontal double-pipe minichannel heat exchanger, Heat Mass Transfer 55 (6) (2019) 1741–1751.

[23] E.I. Jassim, F. Ahmed, Experimental assessment of Al2O3 and Cu nanofluids on the performance and heat leak of double pipe heat exchanger, Heat Mass Transfer 56 (6) (Jun. 2020) 1845–1858, https://doi.org/10.1007/s00231-020-02826-9.

[24] M. Omidi, M. Farhadi, M. Jafari, A comprehensive review on double pipe heat exchangers, Appl. Therm. Eng. 110 (Jan. 2017) 1075–1090, https://doi.org/10.1016/j.applthermaleng.2016.09.027.

[25] M. Awais, A.A. Bhuiyan, S. Salehin, M.M. Ehsan, B. Khan, Md.H. Rahman, Synthesis, heat transport mechanisms and thermophysical properties of nanofluids: a critical overview, Int. J. Thermofluids 10 (May 2021), 100086, https://doi.org/10.1016/j.ijft.2021.100086.

[26] R.R. Riehl, S.M.S. Murshed, Performance evaluation of nanofluids in loop heat pipes and oscillating heat pipes, Int. J. Thermofluids 14 (May 2022), 100147, https://doi.org/10.1016/j.ijft.2022.100147.

[27] B. Kamenik, et al., Numerical analysis of performance uncertainty of heat exchangers operated with nanofluids, Int. J. Thermofluids 14 (May 2022), 100144, https://doi.org/10.1016/j.ijft.2022.100144.

[28] J.P. Meyer, S.A. Adio, M. Sharifpur, P.N. Nwosu, The viscosity of nanofluids: a review of the theoretical, empirical, and numerical models, Heat Transfer Eng. 37 (5) (2016) 387–421.

[29] S.M.S. Murshed, P. Estellé, A state of the art review on viscosity of nanofluids, Renew. Sustain. Energy Rev. 76 (2017) 1134–1152.

[30] H.D. Koca, S. Doganay, A. Turgut, I.H. Tavman, R. Saidur, I.M. Mahbubul, Effect of particle size on the viscosity of nanofluids: a review, Renew. Sustain. Energy Rev. 82 (2018) 1664–1674.

[31] T.X. Phuoc, M. Massoudi, R.-.H. Chen, Viscosity and thermal conductivity of nanofluids containing multi-walled carbon nanotubes stabilized by chitosan, Int. J. Therm. Sci. 50 (1) (Jan. 2011) 12–18, https://doi.org/10.1016/j.ijthermalsci.2010.09.008.

[32] L. Chen, H. Xie, W. Yu, Y. Li, Rheological behaviors of nanofluids containing multi-walled carbon nanotube 32 (4) (Mar. 2011) 550–554, https://doi.org/10.1080/01932691003757223.

[33] A. Banisharif, M. Aghajani, S. Van Vaerenbergh, P. Estellé, A. Rashidi, Thermophysical properties of water ethylene glycol (WEG) mixture-based Fe3O4 nanofluids at low concentration and temperature, J. Mol. Liq. 302 (2020), 112606.

[34] J. Vallejo, J.I. Prado, L. Lugo, Hybrid or mono nanofluids for convective heat transfer applications. A critical review of experimental research, Appl. Therm. Eng. (Dec. 2021), 117926, https://doi.org/10.1016/j.applthermaleng.2021.117926.

[35] M. Awais, et al., Heat transfer and pressure drop performance of nanofluid: a state-of- the-art review, Int. J. Thermofluids 9 (Feb. 2021), 100065, https://doi.org/10.1016/j.ijft.2021.100065.

[36] H.M. Maghrabie, et al., Intensification of heat exchanger performance utilizing nanofluids, Int. J. Thermofluids 10 (May 2021), 100071, https://doi.org/10.1016/j.ijft.2021.100071.

[37] A.G. Olabi, T. Wilberforce, E.T. Sayed, K. Elsaid, S.M.A. Rahman, M.A. Abdelkareem, Geometrical effect coupled with nanofluid on heat transfer enhancement in heat exchangers, Int. J. Thermofluids 10 (May 2021), 100072, https://doi.org/10.1016/j.ijft.2021.100072.

[38] M.J. Assael, K.D. Antoniadis, W.A. Wakeham, X. Zhang, Potential applications of nanofluids for heat transfer, Int. J. Heat Mass Transf. 138 (2019) 597–607, https://doi.org/10.1016/j.ijheatmasstransfer.2019.04.086.

[39] K. Brzóska, B. Jóźwiak, A. Golba, M. Dzida, S. Boncel, Thermophysical properties of nanofluids composed of ethylene glycol and long multi-walled carbon nanotubes, Fluids 5 (4) (2020), https://doi.org/10.3390/fluids5040241.

[40] Y.A. Çengel, J.M. Cimbala, Fluid Mechanics: Fundamentals and Applications, McGraw-HillHigher Education, New York, 2006 [Online]. Available: https://books.google.com.tr/books?id=4RVEAQAAIAAJ.

[41] G.R. Holcomb, A review of the thermal expansion of magnetite, Mater. High Temp. 36 (3) (2019) 232–239.

[42] C. ANSYS, Inc., 'ANSYS CFX-solver theory guide, release 19.1′, pp. 25–26;39, 2019.

[43] Y. Muzychka, M. Yovanovich, Pressure drop in laminar developing flow in noncircular ducts: a scaling and modeling approach, J. Fluids Eng. 131 (11) (2009).

[44] G. Huminic, A. Huminic, Entropy generation of nanofluid and hybrid nanofluid flow in thermal systems: a review, J. Mol. Liq. 302 (2020), 112533.